Analysis of Coupling Effect in Human-Commanded Stiffness During Bilateral Tele-Impedance

Luuk Maria Doornebosch, David A. Abbink, *Senior Member, IEEE*, and Luka Peternel, *Member, IEEE*

***Abstract*—Tele-impedance augments classic teleoperation by enabling the human operator to actively command remote robot stiffness in real-time, which is an essential ability to successfully interact with the unstructured and unpredictable environment. However, the literature is missing a study on benefits and drawbacks of different types of stiffness command interfaces used in bilateral tele-impedance. In this article, we introduce a term called *coupling effect*, which pertains to the coupling between human-commanded stiffness going to the remote robot and force feedback coming from the remote robot. We hypothesize that, whenever the operator's commanded stiffness and force feedback are subject to coupling effect (e.g., muscle activity based stiffness command interfaces), force feedback can invoke involuntary changes in the commanded stiffness due to human reflexes. Although the coupling effect takes away some degree of the operator's control over the commanded stiffness, these involuntary changes can be either beneficial (e.g., during position tracking) or detrimental (e.g., during force tracking) to the task performance on the remote robot side. We examined the coupling effect in an experimental study with 16 participants, who performed position and force tracking tasks by using both coupled type (muscle activity based) and decoupled type (external device based) of interface. The results demonstrate a benefit of the coupling effect when the remote robot is operating in presence of unexpected force perturbations, where lower absolute error in position tracking task was observed. On the other hand, the decoupled type of interface is beneficial for force tracking tasks on the remote robot side, such as establishing or maintaining a stable contact with objects. However, the coupling effect negatively influences the commanding of reference stiffness to the remote robot in both position and force tracking tasks for the coupled type of interface, compared to the decoupled type of interface, which is not affected.**

***Index Terms*—Coupling effect, force feedback, impedance control, stiffness command interface, tele-impedance.**

I. Introduction

TELEOPERATION is usually applied in scenarios where a human-in-the-loop solution is preferred over automation to achieve dexterous interaction with the environment [1]. It also facilitates exploitation of human experiences and cognitive abilities to enable the remote robot to deal with uncertainties and unpredictability of unstructured environmental interactions [2]. Application areas include operating in hazardous environments [3], robot-assisted surgery [4], and teaching robots by demonstration in an intuitive manner [5], [6].

In classic teleoperation, the human controls the remote robot (slave) by solely providing position or velocity inputs [7], where the human has no control over the slave impedance properties. To ensure good position tracking on the slave side, the impedance is preset to a high value by high controller gains [8]. Nevertheless, low impedance may be required to avoid large contact forces when moving in unstructured or unpredictable environments [2], or to facilitate complex manipulation tasks [9], [10]. Furthermore, low impedance can improve stability in force-reflective setups [2], [11]. On the other hand, adaptation from low to high impedance may also be necessary to stabilize the limb [12], [13].

Humans can effectively operate in an unpredictable and unstructured environment, which is partially due to their exceptional cognitive capabilities. However, another key factor compared to traditional robots is the ability of the central nervous system (CNS) to actively regulate mechanical properties of limbs [12], [14]. While human muscles exhibit intrinsic passive viscoelastic properties, these properties can also be actively adapted by the CNS through muscle contraction and cocontraction [14]. This adaptation can be voluntary, but it can also be involuntary and triggered by reflexes. For example, external forces acting on the limb can cause reflexes that induce involuntary muscle activity, which then changes the viscoelastic properties and posture [15]. These important abilities to regulate impedance are absent in classic teleoperation.

In the past decade, classic teleoperation was extended by a concept called tele-impedance [10], which enables the human operator to actively regulate the impedance of the remote slave robot. Initially, the concept was proposed in unilateral teleoperation setup, where the operator could command the impedance in addition to the motion of a robotic arm [5], [10], [16]. In [10], the commanded robot impedance was mapped to the estimated impedance of the operator's arm, which was based on measuring muscle activity in real-time with electromyography (EMG). Even without force feedback, the additional impedance command channel provided a similar performance enhancement as seen in a classic bilateral teleoperation [5], [10]. Nonetheless, tele-impedance with force feedback provides the human operator with much better immersion into the remote environment [2], [17] and becomes crucial when visual feedback is not available [18].

Manuscript received August 3, 2020; revised November 29, 2020; accepted December 11, 2020. Date of publication January 13, 2021; date of current version August 5, 2021. This article was recommended for publication by Associate Editor A. M. Zanchettin and Editor E. Yoshida upon evaluation of the reviewers' comments. *(Corresponding author: Luka Peternel.)*

The authors are with the Haptics Lab of Cognitive Robotics Department, Delft University of Technology, 2628 Delft, The Netherlands (e-mail: luukdoornebosch@hotmail.com; d.a.abbink@tudelft.nl; l.peternel@tudelft.nl).

Color versions of one or more figures in this article are available at https://doi.org/10.1109/TRO.2021.3047064.

Digital Object Identifier 10.1109/TRO.2020.3047064

In literature, there are three main types of methods for commanding the slave robot impedance in real-time that are applied to force feedback tele-impedance setups. In the first method, the human operator regulates the grip force on the handle of the master haptic device in order to command the slave robot impedance [16], [17]. In the second method, the operator uses an external device with a continuous spring-return push button to command the impedance [2], [8]. The third and the most common method employs real-time surface EMG (sEMG) measurements to estimate the human arm impedance, which is then commanded to the remote robot [18], [19].

In this article, we investigate fundamental characteristics of different stiffness commanding interfaces (SCI) in bilateral tele-impedance, and introduce the concept of coupling effect in force feedback tele-impedance. This concept is from now on called *coupling effect* and we define it as *the loss of a degree of control over the commanded stiffness as a result of a neuro-mechanical dependency between force feedback and operator's commanded stiffness*. The commanded impedance sent to the remote robot is a sum of voluntarily impedance changes and involuntarily impedance changes that can result from unexpected force feedback. We categorize interfaces based on biosignals like sEMG measurements [10], [18], [19] or electrical impedance tomography (EIT) [20] as coupled SCIs. Besides voluntarily changes of muscle activity, the sEMG or EIT also measures involuntarily changes in muscle activity due to reflexes induced by unexpected force feedback. This is reflected in the commanded impedance to the remote robot as well. On the other hand, we categorize hand-held external devices [2], [8] that are not affected by force feedback as decoupled SCIs. In such case, involuntary changes of the viscoelastic properties of the operator's limb due to reflexes do not affect the commanded impedance because there is no coupling effect between the force feedback and the stiffness commanding method.

Most of the previous research in tele-impedance used coupled type slave impedance command interfaces [5], [10], [21]. Since they are mostly used in a unilateral teleoperation setup, the coupling effect was not present. Whenever the concept of tele-impedance is used in a bilateral setup [2], [8], [16], [18], [19], the coupling effect becomes important. When a human limb is unexpectedly perturbed, reflexes can cause an involuntary stiffening of the limb [15]. In a coupled SCI, which is based on sEMG or EIT measurements, the measured muscle activity increases when the arm stiffens up in order to counter an unexpected force feedback induced by the bilateral nature of the system. The increased human arm stiffness, as a result of increased muscle activity, simultaneously affects the stiffness of the slave robot through the impedance command channel. This hypothetically causes a temporal mismatch between the intended slave stiffness (required to perform a given task) and the actual commanded slave stiffness. While this temporal stiffness mismatch due to the coupling effect takes away some degree of operator's control over the remote robot impedance, it might not necessarily negatively affect the task performance on the robot side. For example, if the remote robot experiences undesired perturbations, the force feedback might make the human to naturally stabilize the remote robot through the coupling effect.

Based on the abovementioned condition, we hypothesize the following.

1) *H1:* The force feedback negatively affects tracking of the desired commanded stiffness in a coupled type of interface, while it has no effect in a decoupled type of interface.
2) *H2:* The coupling effect between force feedback and commanded stiffness helps a position tracking task in case of unexpected perturbations when using a coupled type of interface.
3) *H3:* The coupling effect between force feedback and commanded stiffness negatively affects a force tracking task in case of physical interaction when using coupled type of interface.
4) *H4:* The coupling effect has a larger negative effect on commanded stiffness when maintaining a reference contact force compared to establishing contact in case of physical interaction.

To test these hypotheses, we design an experiment consisting of two tasks that the operator has to perform at the remote robot.

1) Track the reference position in presence of random perturbations, from now on called *position tracking task*.
2) Establish a contact with an unknown object and maintain reference interaction force, from now on called *force tracking task*.

These tasks represent two fundamental types of interaction with the unstructured and unpredictable environment, where adjusting impedance is crucial. We test two main experiment conditions (stiffness commanding with a coupled and decoupled interface) in these two tasks.

A short preliminary study was submitted to [22]. The study, in this article, significantly extends the preliminary study by a considerably more through theoretical formulation of the concept and methodology (including transparency and stability analysis); by several novel experiment results; and by a novel discussion and scientific findings. Novel experiment results include: a subjective analysis, deeper analysis of different phases of interaction tasks (i.e., contact establishment versus contact maintenance), and an analysis regarding the effect of the double task performance (i.e., primary position/force tracking and secondary stiffness tracking).

II. Theoretical Background

In this study, the novel concept of coupling effect is analyzed on a fundamental level in a clean condition. If the study was conducted in unpredictable and variable conditions with real-world teleoperation issues, it would be difficult to determine whether the particular results were caused by the coupling effect or any of the other conditions and issues. Therefore, we deliberately made the choice to avoid some of the real-world bilateral teleoperation issues (i.e., time delay, stability, and transparency), which could influence/corrupt the results of the coupling effect. In other words, we wanted to isolate the coupling effect to examine its specific influence on a fundamental level. To do so, we used a simulated impedance-controlled slave robotic manipulator and remote environment, which were generated on the same

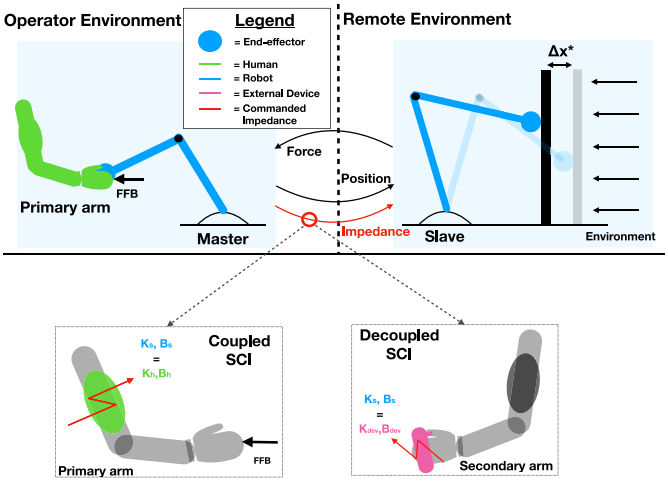

Fig. 1. Concept of bilateral tele-impedance. According to the impedance control law, the force feedback (FFB) felt by the human operator is calculated by (1). This FFB depends on the difference between desired (or commanded) and actual slave robot position in combination with the commanded stiffness. Whenever the environment presses against the slave robot, the magnitude of the deviation from commanded position depends on the commanded impedance. The difference of the slave robot end-effector position induced by a constant environmental force between high and low commanded stiffness is indicated by Δx. The stiffness and damping are estimated from the operator's primary limb properties (i.e., the limb which controls the master robot) when the impedance is commanded by a coupled SCI. In a decoupled SCI, the impedance is commanded via an external device operated by the operator's secondary limb (i.e., a limb which does not control the master robot).

computer that was used for control of the haptic device hardware. Nevertheless, transparency and time delay issues can be effectively solved by the various method and solutions from the literature [7], [11], [18], [23]–[25]. For analysis of transparency and stability that highlights specific aspects of the coupling effect introduced in this study, we refer to Appendix.

It is also important to stress that our primary focus was on examining performance of the human operator on the remote robot side since that is where the actual task exists. The focus is not on effects of neuro-mechanical aspects on the human operator's side, since this dependency is a side effect from the coupled SCI's design. Since the decoupled SCI does not have such a side effect, the comparison can only be made with respect to the task performance on the remote robot side.

A. Tele-Impedance Control

The study involved the bilateral tele-impedance methods illustrated in Fig. 1. The human operator commanded the motion and impedance parameters of the remote robot (slave) through two different types of interfaces (in our case coupled and decoupled SCI), while in return received force feedback from the remote environment. According to the impedance control law [26], the external interaction force of remote robot depends on the impedance parameters and the difference between reference and actual position/motion as

$$\boldsymbol{f}_{\text{ext}} = \boldsymbol{K}(\boldsymbol{x}_d - \boldsymbol{x}_a) + \boldsymbol{D}(\dot{\boldsymbol{x}}_d - \dot{\boldsymbol{x}}_a) \tag{1}$$

where $\boldsymbol{f}_{\text{ext}} \in \mathbb{R}^6$ is the external force acting from the remote robot on the remote environment. Vector $\boldsymbol{x}_a \in \mathbb{R}^6$ is the actual slave robot end-effector position and vector $\boldsymbol{x}_d \in \mathbb{R}^6$ is the desired end-effector position. $\boldsymbol{K} \in \mathbb{R}^{6\times6}$ and $\boldsymbol{D} \in \mathbb{R}^{6\times6}$ indicate the commanded stiffness and damping matrix, respectively. To keep the output bounded and stable, the damping term is included. The master velocity is not controlled as there is no predefined velocity trajectory to be followed. This simplifies (1) to

$$\boldsymbol{f}_{\text{ext}} = \boldsymbol{K}\Delta\boldsymbol{x} - \boldsymbol{D}\dot{\boldsymbol{x}}_a \tag{2}$$

where $\Delta\boldsymbol{x} = \boldsymbol{x}_d - \boldsymbol{x}_a \in \mathbb{R}^6$ indicates a displacement between the desired and actual position [27].

B. Human Limb Stiffness

The human limb's endpoint stiffness depends on posture and viscoelastic limb properties. There are various biomechanical studies that provide stiffness measurements [28]–[30], as well as models that provide the relationships between relevant variables [31]–[33]. The endpoint stiffness matrix can be calculated form the joint stiffness matrix as

$$\boldsymbol{K} = \boldsymbol{J}^{-T}(\boldsymbol{q})\boldsymbol{K}_J\boldsymbol{J}^{-1}(\boldsymbol{q}) \tag{3}$$

where $\boldsymbol{K} \in \mathbb{R}^{6\times6}$ is the endpoint stiffness matrix and $\boldsymbol{K}_J \in \mathbb{R}^{n\times n}$ is the joint stiffness matrix, with n being the joint-space degrees of freedom (DoF). The postural dependency is captured by the limb Jacobian $\boldsymbol{J}(\boldsymbol{q}) \in \mathbb{R}^{6\times n}$, where $\boldsymbol{q} \in \mathbb{R}^6$ is the joint configuration vector. According to the Hill's muscle model, individual muscle consists of an active contractile element (CE) and two passive elements; a series element (SE), and a parallel element (PE) [34]. This results in a generalized muscle stiffness as a function of the contributions of these elements

$$\boldsymbol{K}_m(\boldsymbol{a}, \boldsymbol{q}) = \mu(\boldsymbol{K}_{\text{SE}}, \boldsymbol{K}_{\text{PE}}, \boldsymbol{K}_{\text{CE}}) \tag{4}$$

where $\boldsymbol{K}_m \in \mathbb{R}^{m\times m}$ is the muscle stiffness, which is a function (μ) of the stiffness contributions of the CE, the SE and the PE $\boldsymbol{K}_{\text{CE}}$, $\boldsymbol{K}_{\text{SE}}$, $\boldsymbol{K}_{\text{PE}}$, respectively [34]. Vector $\boldsymbol{q}$ denotes postural dependency and vector $\boldsymbol{a} \in \mathbb{R}^m$ denotes muscle-activity dependency, with m being number of muscles.

Contribution of passive elements can be neglected if both muscle and tendon are far from stretched or compressed limits, meaning that the muscle stiffness matrix estimation solely depends on active regulation [21]. From the muscle stiffness matrix the joint stiffness can be obtained as

$$\boldsymbol{K}_J = \boldsymbol{J}_m^T(\boldsymbol{q})\hat{\boldsymbol{K}}_m(\boldsymbol{a})\boldsymbol{J}_m(\boldsymbol{q}) \tag{5}$$

where $\hat{\boldsymbol{K}}_m \in \mathbb{R}^{m\times m}$ is the estimated muscle stiffness matrix. Matrix $\boldsymbol{J}_m(\boldsymbol{q}) \in \mathbb{R}^{m\times n}$ represents muscle Jacobian, which is also configuration dependent [35]. Equation (5) in turn can be substituted in (3) to obtain the endpoint stiffness profile. Besides these simplifications, estimation of $\hat{\boldsymbol{K}}_m$ remains a convoluted process. In [10], efforts were carried out to estimate this term from muscle activity and posture measurements. To reduce complexity, several simplified methods were proposed in [14] and [36]–[39].

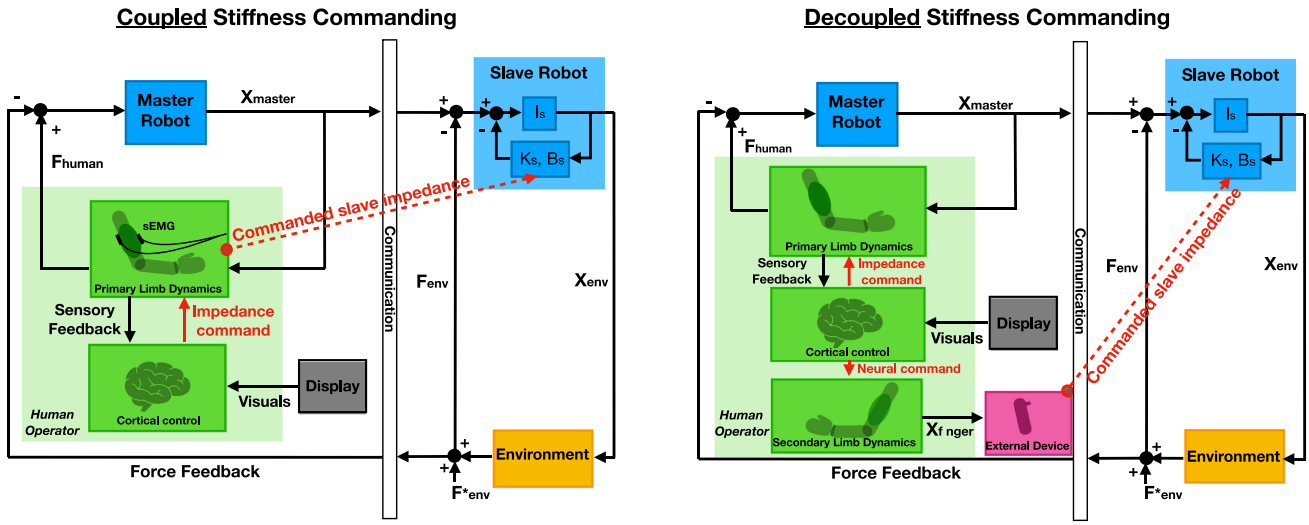

Fig. 2. Block schemes of a force feedback tele-impedance setup for a coupled SCI (left) and a decoupled SCI (right). The primary limb refers to the limb holding the master robot (i.e., haptic interface). The secondary limb does not control the master robot but is the free limb and is able to hold an external device for stiffness commanding. When a coupled SCI is used, the human endpoint impedance profile is estimated from the primary limb dynamics and is sent to the slave robot. Next to the passive limb properties, the primary limb dynamics can be altered by voluntary muscle contraction from cortical control based on visual information from the remote environment, where the task is. In addition, reflexes can also involuntarily cause muscle contractions, which alter the primary limb dynamics too. These spinal reflexes can be induced by the force feedback of the system. For simplicity, this complex spinal reflex loop is included in the primary limb dynamics block. When stiffness and damping are commanded by a decoupled SCI, the impedance is determined by the finger position (X_{finger}), which controls the external device. This is solely dependent on visual feedback and task requirements. Subscript env correspond to the remote environment. X, F and K correspond to position, force and stiffness respectively. The star superscript indicates that the force is external. In the coupled SCI, estimated human arm impedance is equal to the slave robot impedance ($K_s = K_h$). In the decoupled SCI, $K_h \neq K_s$ and $K_s = K_{\text{device}}$, because the impedance is manually commanded by a finger solely based on visual information from the environment.

The essence of the coupling effect can be captured by looking at the stiffness trend index determined from sEMG signals of two easily accessible and dominant muscles [18], [36], [38], [39]. The posture dependency is neglected as the operator's arm stays within a redundant manifold of the starting configuration [21], [40], therefore, the endpoint stiffness matrix $\boldsymbol{K}$ estimation depends on the muscle activation level of the dominant muscle pair according to [21]. In our study, we were interested in the stiffness estimation and commanding in a single degree of freedom, therefore, the matrix was simplified into a scalar (see Section III-C for details).

C. Theoretical Examination of Coupling Effect

Fig. 2 illustrates a bilateral tele-impedance block scheme for the coupled (left) and decoupled (right) SCI. In the coupled condition, the slave robot stiffness is commanded by the stiffness estimation from the primary limb of the human operator. The primary limb is the arm that controls the master robot (i.e., haptic interface). The primary limb stiffness, as described in (3)–(5), is affected by voluntary changes due to visual cues from the remote environment, where the task is preformed through the remote robot, and by the force feedback at the master robot. Due to the bilateral nature of the setup, force feedback can also induce unexpected movement of the master robot. Such abrupt changes can induce involuntary stiffness changes of the primary limb due to human reflexes captured by the coupling effect. In the decoupled condition, the slave robot stiffness is solely determined by the operator's voluntary stiffness input based on visual cues from the remote environment, since the slave stiffness is commanded via an external device. This external device is not influenced by the primary limb stiffness, since it is controlled by the secondary limb that does not interact with the master robot.

Based on (2), we defined the control law for the coupled and decoupled interfaces as

$$\boldsymbol{f}_C = \boldsymbol{K}(\text{vc}, \text{ic})(\boldsymbol{x}_d - \boldsymbol{x}_a) - \boldsymbol{D}\dot{\boldsymbol{x}}_a \tag{6}$$

$$\boldsymbol{f}_D = \boldsymbol{K}(\text{vc})(\boldsymbol{x}_d - \boldsymbol{x}_a) - \boldsymbol{D}\dot{\boldsymbol{x}}_a \tag{7}$$

where $\boldsymbol{f}_C$ and $\boldsymbol{f}_D$ are the interaction forces acting from the remote robot to the remote environment in a coupled and decoupled scenario, respectively. In case of a coupled SCI, the commanded stiffness $\boldsymbol{K}$ is a function of voluntary operator commands (vc) and involuntary operator commands (ic) due to reflexes caused by the force feedback. In case of a decoupled SCI, stiffness is only a function of voluntary operator commands, since force feedback does not influence external SCI operated by the secondary limb.

Damping matrix was used to stabilize the system and was defined as a function of the commanded stiffness matrix as

$$\boldsymbol{D} = 2 \cdot \zeta \cdot \sqrt{\boldsymbol{K}} \tag{8}$$

where ζ is a damping coefficient, which was set to 0.7 [41]. This makes the system critically damped, which helps to return it into the equilibrium as quickly as possible without large overshoots and oscillations.

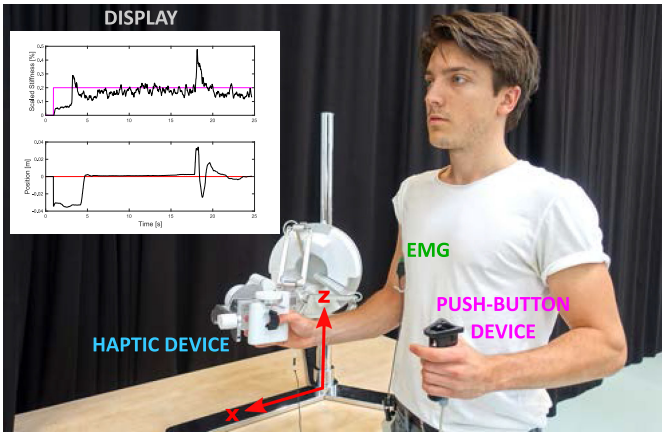

Fig. 3. Illustration of experiment setup. The participant controlled the Sigma.7 haptic device with the right arm, whose movement was constrained in translation and rotation for all axes except for translation along the x-axis. The participant commanded the remote robot stiffness either with EMG measurements as coupled SCI or the push-button device as decoupled SCI. In the coupled scenario, we used two electrodes of the Delsys Bagnoli EMG-system and were connected to the Bicep Brachii and the Tricep Brachii on the right arm. In the decoupled scenario, the participant operated the push-button device with the left hand. In the position tracking task, the participant watched a display showing time traces of the commanded scaled stiffness and virtual slave position. A time trace of the virtual slave force was additionally provided in the force tracking task.

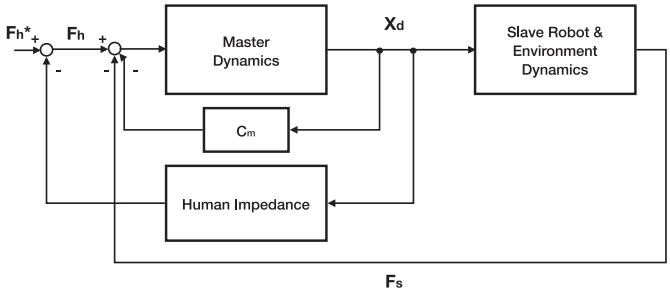

Fig. 4. Block scheme depicts the position-force bilateral teleoperation control architecture of experiment setup. F_h^* is the voluntarily applied force by the human, F_h is the force applied on the master robot. x_d is the commanded master position, which is the reference for the slave robot. C_m is the local controller of Sigma.7 device at the master side, which provides gravity compensation and constrains all DoFs except translation in x-axis. Interaction with the environment (perturbation or pressing against a wall) is simulated as a change in slave dynamics according to Fig. 5.

III. Methods

We compared two stiffness command methods. For the coupled SCI, we used a simplified version of the method in [21] that is based on measuring muscle activity by sEMG. For the decoupled SCI, we used the method in [2] that is based on a push-button device. The two methods were compared to each other in a position tracking task and a force tracking task, resulting in four main experiment trials.

A. Participants

In total, 16 participants (1 woman and 15 men) between 23 and 54 years old ($M = 25.9$, SD $= 7.5$) participated in the experiment. None of the participants had experience with teleoperation. Their participation was voluntary and their efforts were not financially compensated for. All experiment protocols were approved by the Human Research Ethics Committee of TU Delft (approval nr. 874) and all research was performed in accordance with relevant guidelines and regulations. All subjects gave a written informed consent prior to their participation.

B. Experiment Setup

The experiment setup is shown in Fig. 3. We used a 7 DoF Force Dimension Sigma.7 haptic device to teleoperate a simulated remote robot. We examined translational movements in x-axis and constrained movements in other axes. This means that the participant could only move the device forward and backward. Impedance control was implemented in both experiment tasks for both conditions [see (6) and (7)]. A monitor was used to display commanded and reference signals in real-time. In both tasks, reference stiffness and current commanded stiffness were both displayed on one graph, while the remote robot's actual position was displayed on the other graph. A graph that showed interaction force was additionally provided solely in the force tracking task. The participant had to follow reference position in the position tracking task and reference force in the force tracking task, in addition to the reference stiffness. In the position tracking task, the reference position was additionally displayed in the position graph. In the force tracking task, the reference contact force was additionally displayed in the force graph.

In this study, we used a simplified version of a position-force bilateral teleoperation control architecture [42] (see Fig. 4). For the reason mentioned at the beginning of Section II, the system was perfectly transparent [7] and only negligible time delays were present in this study. Performing this study under these clean circumstances was desirable since we focused on investigating the concept of the coupling effect on a fundamental level. The Sigma.7 master robot could freely move along the unconstrained x-axis and its gravity was compensated. Interaction was simulated by changing the virtual slave dynamics during the particular interaction period, which will be discussed in more detail in Section III-D.

C. Commanded Slave Stiffness

For the coupled SCI, we used sEMG-based muscle activity measurement by the Delsys Bagnoli system. As in [21] and[38], we used the Bicep Brachii and Tricep Brachii antagonistic muscle pair to estimate the human arm stiffness trend. Sensor contacts consisting of two silver bars (10 $\times$ 1 mm diameter of 10 mm contact spacing) were placed over the Bicep Brachii short head and Tricep Brachii lateral head. Electrodes were placed in the direction of the muscle fibers. The ground electrode pad was placed on the wrist. Furthermore, skin conduction was improved by local shaving of skin and cleaning with alcohol. The abovementioned process was done according to SENIAM standards [43]. Raw EMG signals were preamplified by the main amplifier of the Delsys Bagnoli EMG system with a gain of 1000. The signal was sampled at 1 kHz with a National Instruments DAQ device. During the real-time processing, the signal was

first high-pass filtered (second order, cutoff frequency 20 Hz) to obtain zero mean and then rectified before we applied a low-pass filter (second order, cutoff frequency 2 Hz) to obtain its envelope.

We defined the commanded slave stiffness K_s for both coupled and decoupled SCI as

$$K_s = \alpha K_{\max} \tag{9}$$

where $K_{\max}$ is the maximum possible controllable stiffness of the remote robot, which is scaled by an interface control factor α. In case of the coupled SCI, we calculated it as

$$\alpha_c = K \cdot s_K \tag{10}$$

where α_c is the coupled scaling factor that depends on the current stiffness trend estimation based on cocontraction

$$K = \frac{a_b + a_t}{2} \tag{11}$$

where muscle activation for Biceps a_b and Triceps a_t were obtained by normalizing processed EMG signals to their maximal voluntary contraction (MVC) as

$$0 \leq a_b(t) = \frac{\mathrm{EMG}_b(t)}{\mathrm{MVC}_b} \leq 1 \tag{12}$$

$$0 \leq a_t(t) = \frac{\mathrm{EMG}_t(t)}{\mathrm{MVC}_t} \leq 1. \tag{13}$$

We used parameter s_K in (10) to select the muscle activation range used for the stiffness commanding. Since high cocontraction is physically very demanding and cannot be maintained for a longer period, the upper range is not practical for using it to control the stiffness of the remote robot. Therefore, in our case we set $s_k = 0.5$, which would correspond to 50% of maximum cocontraction.

In case of the decoupled SCI, we calculated the control factor as

$$\alpha_d = \frac{V}{V_{\max}} \tag{14}$$

where α_d is the decoupled scaling factor that depends on voltage V of potentiometer, which was controlled by the current position of the spring-return button. Normalization was done based on the maximum voltage $V_{\max}$. From here on forward the spring-return linear potentiometer used as decoupled SCI is called *push-button device*.

Both sEMG and push-button signals were sampled at 1 kHz by a National Instruments DAQ device (USB-6002). These signals, as well as the force and position measurements from Sigma.7 (sampled at 100 Hz), were processed in C++ and sent to MATLAB/Simulink via UDP packages (local host), to be displayed to the participant in real-time plots.

D. Experiment Protocol

Before the experiments, each participant performed MVC of the relevant muscles used in this experiment. During the experiments, the participants took a standing pose in front of the Sigma.7 master robot. The height of the Sigma.7 was adjusted so that it was held comfortably at 90° of elbow flexion (see Fig. 3).

TABLE I
NUMBER IS ALLOCATED TO THE TWO TASKS WITH TWO STIFFNESS COMMAND INTERFACE CONDITIONS

	Position Task	Force Task
Coupled SCI	Training	Training
	1	3
Decoupled SCI	Training	Training
	2	4

TABLE II
COUNTERBALANCED CONDITION ORDER PER PARTICIPANT GROUP

Participant	Conditions			
$4i-3$	1	2	4	3
$4i-2$	2	3	1	4
$4i-1$	3	4	2	1
$4i$	4	1	3	2

Here, $i = 1$, 2, 3, and 4.

Each participant was first familiarized with the stiffness commanding methods during pretrials, where a reference stiffness signal was followed using both SCIs. The reference stiffness signal in the familiarization pretrials was identical for both SCIs and consisted of four step functions and a chirp signal of two periods. The value ranged between 4% and 25% of the coupled and decoupled scaling factors as defined in (10) and (14). To minimize the effects of learning, additional training trials were performed before every task. The training trial was similar to that of the task trial, except that different representable dependent variables were chosen.

The experiment used a repeated measures design. We tested every participant in two tasks with two different SCIs for five repetitions. The SCI refers to which system was used by the participant to command the stiffness to the remote robot and perform the task in the remote environment. The coupled SCI used the participant's sEMG measurements to command the stiffness, while the decoupled SCI used the push-button device. This resulted in four combinations of task and SCI. We randomized the order in which the participants received the conditions based on a balanced Latin Square. This was done to keep the participants as engaged as possible and to further mitigate effects of learning. The two tasks are shown in Table I and the subdivision of the 16 participants in four groups with the corresponding task order is shown in Table II. We defined the tasks that had to be performed through the teleoperated robot in the remote environment as:

Position tracking: The participant was asked to move the Sigma.7 to the reference position and keep it there. When this reference position was reached, the participant tried to maintain the reference stiffness (through either coupled or decoupled SCI), while simultaneously keeping the reference position. The primary goal of the participant was to maintain this reference position as well as possible. After the force perturbation at a random time, the participant had to bring the robot back to the reference position and command the correct stiffness according to the reference.

Force tracking: The participant was asked to move the Sigma.7 towards them (in front of the virtual wall). The virtual wall would appear after 15 s (for safety reasons). When the wall

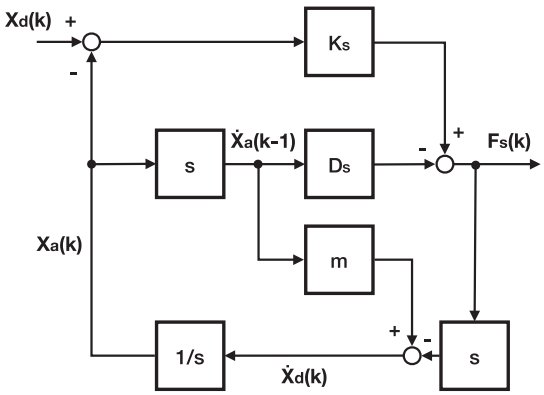

Fig. 5. Detailed block scheme of the slave and environment dynamics block of Fig. 4. F_s is the remote robot force, k is the current time step, x and $\dot{x}$ are the position and velocity, respectively. K_s and D_s are stiffness and damping of the remote robot (slave), respectively. Subscript a, d, and s indicate actual, desired and slave, respectively. The blocks s and $1/s$ represent derivation function and integrator function, respectively. Mass of an object that collides with and perturbs the remote robot is marked with m.

appeared the participants were given a verbal conformation from the experimenter. When the participant comfortably maintained the reference stiffness, he/she approached the wall to establish a stable contact and then tried to maintain the reference interaction force of 10 N and reference stiffness simultaneously. The primary goal of the participant was to maintain this reference interaction force as well as possible.

The force feedback for each task was designed as follows.

Perturbation: While the participant was tracking the position and the stiffness reference, a perturbation occurred at a random time. We determined the parameters of imposed perturbation by a preliminary pilot study. The aim was to find moderate perturbation intensity, in order not to perturb beyond human capacity to handle, and to be strong enough to present a reasonable challenge in position tracking task. This perturbation force was equivalent to a mass of 5 kg hitting the impedance-controlled virtual remote robot with a velocity of $1\frac{m}{s}$. We used conservation of momentum principle to calculate the states of the slave robot as

$$x_a(k) = x_a(k-1) + \dot{x}_a(k-1)dt \tag{15}$$

$$F(k) = K_s(k)\big(x_d(k) - x_a(k)\big) - D_s(k)\dot{x}_a(k-1) \tag{16}$$

$$\dot{x}_a(k) = m\dot{x}_a(k-1) - F(k)dt \tag{17}$$

where k indicates the current step, m is the mass of the virtual object hitting the virtual slave, F is the interaction force between the two, while x and $\dot{x}$ are position and velocity of the slave, respectively. Subscript s, a, and d represent slave, actual, and desired, respectively. The desired position x_d was the commanded position as measured by the Sigma.7 master robot, while the slave stiffness K_s was commanded by either the coupled or decoupled SCI in real-time according to (9). D_s is the commanded damping calculated by (8). Time step dt was set to 0.01 s. Conservation of momentum principle in combination with impedance control is shown in Fig. 5. This force perturbation F lasted for one second at the slave robot side and was fed back and replicated in real-time at the master robot held by the participant. The reference stiffness signal was set at 20% of the maximum virtual slave robot stiffness ($K_{\max} = 500\ \frac{N}{m}$).

Virtual wall: When the participant initiated forward movement while tracking stiffness reference, a contact with the wall was established at $x = 0.015$ m. The reference stiffness signal was set at 20% of the maximum virtual slave robot stiffness ($K_{\max} = 2000\frac{N}{m}$). The force feedback due to impedance control was felt by the participant when the contact was established with the wall according to (16). The virtual wall was implemented as a constraint on the actual position when $x > 0.015$ m, therefore, $\dot{x}_a = 0$ was set at the contact as further motion was not possible.

E. Dependent Measures

We analyzed position, force, and stiffness signals during the period of force feedback. For analysis of the position tracking task, we aligned the datasets of the repetitions at the moment when the force perturbation occurred. For analysis of the force tracking task during the contact establishment (or pressing) period [0–10] N, we aligned the datasets of the repetitions at the moment of contact with the wall. For analysis of maintaining the reference interaction force with the wall, we aligned the datasets of the repetitions at the instance when 10 N reference force was first crossed. In each case, we looked at the primary (position or force) and secondary (stiffness) task performance, effect of double task performance (i.e., simultaneous position/force tracking and stiffness tracking), and subjective results from a questionnaire.

Task performance: We quantified task performance as the average over the mean absolute error between signal and reference signal of the five repetitions. In the following definitions subscripts err and ref are error and reference, respectively. Furthermore, T is generally used as the length of the corresponding time-vector. For the position tracking task during the force perturbation (lasting 1 s), we used the following metrics.

1) Mean absolute position error [m]: $\bar{x}_{\text{err}} = \frac{\sum |x_a - x_{\text{ref}}|}{T}$.
2) Mean absolute stiffness error [-]:[1] $\bar{\alpha}_{\text{err}} = \frac{\sum |\alpha - \alpha_{\text{ref}}|}{T}$. For the force tracking task using the contact with the wall (reference force of 10 N for 4 s),[2] we used the following metrics.
3) Mean absolute force error [N]: $\bar{F}_{\text{err}} = \frac{\sum |F - F_{\text{ref}}|}{T}$.
4) Mean absolute stiffness error [-][1]: $\bar{\alpha}_{\text{err}} = \frac{\sum |\alpha - \alpha_{\text{ref}}|}{T}$.

The mean absolute stiffness error was additionally used to quantify the difference in stiffness tracking performance between establishing contact period (i.e., pressing from [0 to 10] N) and maintaining contact (10 N) for 4 s with the wall.

Double task effect: To provide an insight in how double task performance (i.e., simultaneous position/force tracking and stiffness tracking) affects both SCIs, we used the following metrics.

[1]These are unitless variables since the stiffness scaling factor α was normalized by MVC and by maximum potentiometer voltage for coupled and decoupled SCI, respectively.

[2]The individual observation window of 4 s only started after the reference force 10 N was reached.

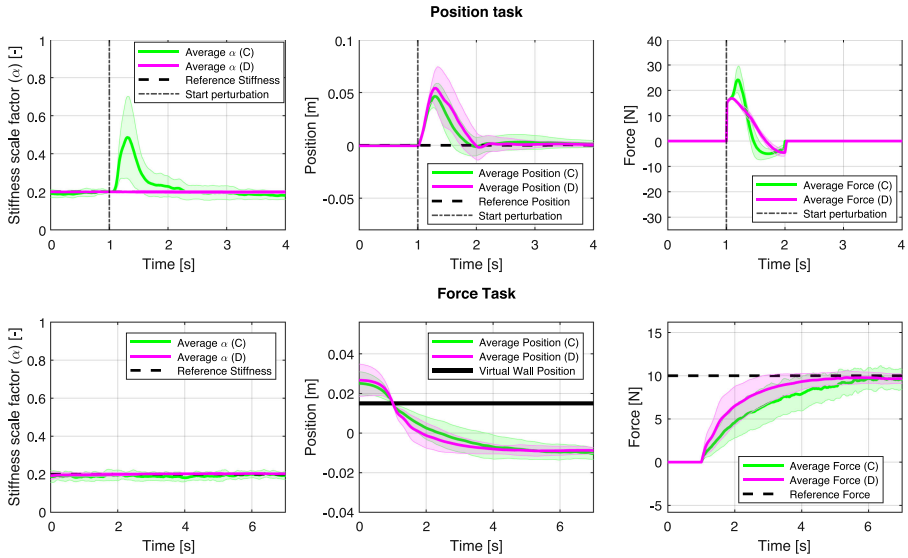

Fig. 6. Average values over all 16 participants in the position tracking task (top row) and the force tracking task (bottom row). The results from the coupled SCI (green) condition and the decoupled SCI (magenta) condition are plotted on top of one another for both tasks. A cloud of one SD is plotted around the average. The displayed position in the force task graph is the commanded slave position (i.e., equal to the master position).

1) RMSE of the position [m] before the perturbation occurs: $\bar{x}_{\text{RMSE}} = \sqrt{\frac{\Sigma(x_a - x_{\text{ref}})^2}{T}}$. This indicates reference following performance.
2) Mean time to reference force [s]: MTTR $= T_{10N} - T_{0N}$. Here, T_{10N} and T_{0N} are time stamps indicating the crossing of force values 10 N and 0 N, respectively. This rise time (MTTR) indicates the time it took the participant to press from 0 to 10 N.

This effect was observed in the period prior to perturbation for the position tracking task and in the period prior to maintaining a stable force with the wall for the force tracking task. In these periods, the participants could focus more on simulations primary and secondary task performance at the remote robot. After those periods, however, the primary task performance became dominant.

Subjective analysis: Participants provided answers on the following questions.

1) *Q1:* "Which stiffness command interface was more convenient in controlling the reference stiffness in terms of comfort?"
2) *Q2:* "Did you feel that the muscle interface helped you to counteract the perturbation and maintain the desired position?"
3) *Q3:* "Did you feel that using the push-button interface helped you to keep the reference force on the wall?"

F. Statistical Analyses

For statistical analyses, we performed paired sample t-tests. The datasets were checked for normality by performing the Anderson-Darling test. If the dataset did not pass this test, non-normal distributed data was corrected by a rank-transformation before hypothesis testing [44]. Because we conducted two analyses on the dataset corresponding to maintaining contact force with the wall, while commanding reference stiffness, we applied a Bonferroni correction, which compensated for the increased chance of committing a Type I error [45].

IV. Results

Fig. 6 shows the average results of all 16 participants for position tracking and force tracking and also provides an overview of the effect of force feedback on the commanded stiffness in different tasks. The period of familiarization with the task during the training trials was not analyzed. The coming paragraphs show results regarding the effect on commanded stiffness, position tracking, and force tracking for different SCIs.

A. Coupling Effect on Commanded Stiffness

Table III shows the mean and standard deviation (SD) for all dependent measures. In addition, the results of the paired-sample t-tests are reported. In the position tracking and force tracking tasks the commanded stiffness in a coupled SCI is influenced by the two different force feedback scenarios (perturbation and maintaining a contact). The left column graphs of Fig. 6 show time-series plots related to commanded stiffness for both commanding methods and for both tasks. Fig. 7 shows the mean absolute stiffness error in both tasks during the force feedback duration.

First, comparison of the absolute mean commanded stiffness error in the position tracking task between the coupled SCI and decoupled SCI yielded a higher error when the coupled SCI was used. The difference was statistically significant $t(15) = 9.66$, $p \leq 0.001$. Second, comparison of the absolute mean commanded stiffness error in the force tracking task between the coupled SCI and decoupled SCI again yielded a higher error when the coupled SCI was used. The difference was statistically significant $t(15) = 11.54, p \leq 0.001$. Finally, comparison of the

TABLE III
MAIN RESULTS OF STATISTICAL ANALYSIS

Position Task		Coupled SCI M, (SD)	Decoupled SCI M, (SD)	t(df), p-Value
Task Performance Keeping ref. position	Mean absolute position error [m]	.0242, (.0082)	.0295, (.0117)	$t(15) = -2.97,\ p = 0.0096^{*}$
	Mean absolute stiffness error [-]	.1194, (.0740)	.0061, (.0041)	$t(15) = 9.66,\ p \leq 0.001^{*}$

Force Task		Coupled SCI M,(SD)	Decoupled SCI M,(SD)	t(df), p-Value
Task Performance Keeping 10N ref. force	Mean absolute force error [N]	1.1218,(.3109)	0.4303,(0.3413)	$t(15) = 7.45,\ p \leq 0.001^{*}$
	Mean absolute stiffness error [-]	.0277,(.0082)	.0067,(.0037)	$t(15) = 11.54,\ p \leq 0.001^{*,**}$

		Pressing 0-10N M,(SD)	Pressing 10N constant M,(SD)	X / X	
Task Performance Pressing 0-10N vs. Keeping 10N ref. force	Mean absolute stiffness error [-]	.0277,(.0075)	.0277,(.0082)	X	$t(15) = -0.0126,\ p > 0.05$

Means (M), standard deviations (SD) and effect sizes of the t-tests are calculated per metric. Superscript * indicates that the dataset did not pass the Anderson-Darling test (normally distributed), therefore the dataset was rank-transformed before the statistical test was performed. Superscript ** indicates that a Bonferroni correction was applied to prevent Type I error.

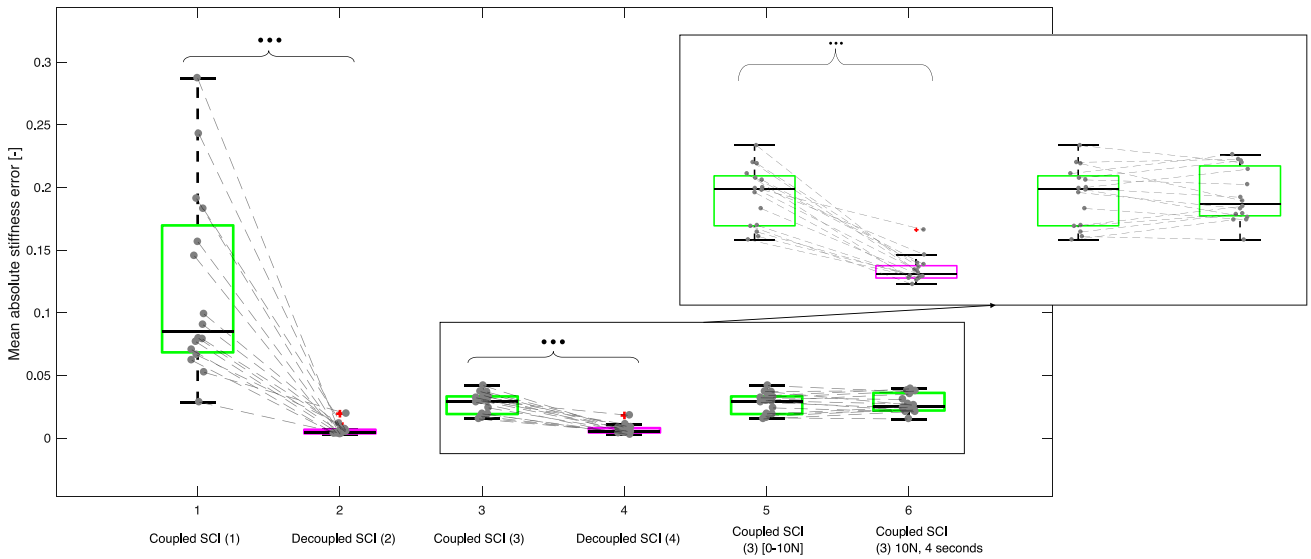

Fig. 7. Reference stiffness tracking in two tasks for the four conditions (1), (2), (3), (4) (see Table I). Boxplots of the mean absolute error of the deviation from the reference stiffness during the perturbation (position tracking task) is depicted on the left-most side. The mean absolute stiffness error during maintaining 10 N force for 4 seconds with the virtual wall (force tracking task) is depicted in the middle. In addition, a comparison between the period of pressing from 0 to 10 N and the period of maintaining 10 N is given for the coupled condition on the right side. The coupled SCI is indicated by green color and the decoupled SCI by magenta color. Result of each individual participant is indicated by a grey dot. The within subject difference is represented by the grey dotted lines connecting the dots. The black dots (● ● ●), (●●), (●) indicate a significance level of $p \leq 0.001$, $p \leq 0.01$, $p \leq 0.05$, respectively.

absolute mean commanded stiffness error with the coupled SCI in the force tracking task during the period of pressing from 0 to 10 N and maintaining 10 N force for 4 s yielded no statistically significant difference $t(15) = -0.013$, $p > 0.05$.

B. Coupling Effect on Position Tracking

In the position tracking task, we compared the mean absolute error from the reference position during the perturbation between the two SCIs. Comparison of the mean absolute position error in the position tracking task between the coupled SCI and decoupled SCI yielded a higher error when the decoupled SCI was used. The difference was statistically significant $t(15) = -2.97$, $p = 0.0096$. This is depicted in Fig. 8(a) and shown in Table III. The top-row graphs of Fig. 6 show time-series plots related to position tracking for the coupled SCI and the decoupled SCI.

C. Coupling Effect on Force Tracking

In the force tracking task, we compared the mean absolute error from the reference force during maintaining 10 N force for 4 s with the virtual wall. Comparing the mean absolute force

TABLE IV
DOUBLE TASK PERFORMANCE ANALYSIS

		Coupled SCI	Decoupled SCI	t(df), p-Value
Position Task		M,(SD)	M,(SD)	
Effect of double task	RMSE of the position [m]	.0020, (5.6069e-04)	.0013, (3.9494e-04)	$t(15) = 3.68$, $p = .0022$
		Coupled SCI	Decoupled SCI	t(df), p-Value
Force Task		M,(SD)	M,(SD)	
Effect of double task	Mean time to reference force [s]	3.4105, (1.4661)	2.4886, (1.0395)	$t(15) = 2.45$, $p = .0268$

Means (M), standard deviations (SD) and effect sizes of the t-tests are calculated per metric. Superscript * indicates that the dataset did not pass the Anderson-Darling test (normally distributed), therefore the dataset was rank-transformed before the statistical test was performed. Superscript ** indicates that a Bonferroni correction was applied to prevent Type I error.

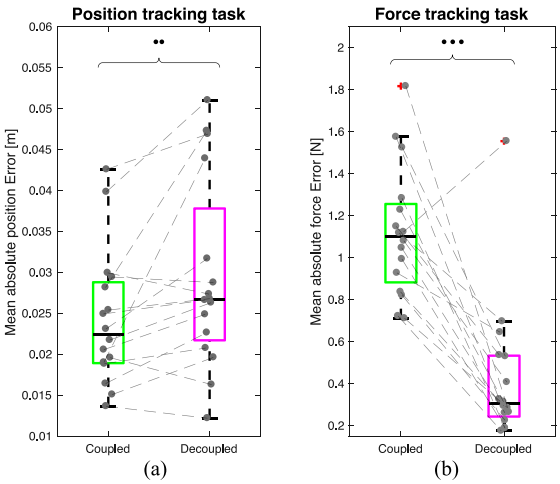

Fig. 8. (a) Mean absolute error of the deviation from the reference position during the force perturbation. (b) Mean absolute error of the deviation from the reference force during maintaining 10 N force for 4 s with the virtual wall. The coupled SCI is indicated by green color and the decoupled SCI by magenta color. Result of each individual participant is indicated by a grey dot. The within subject difference is represented by the grey dotted lines connecting the dots. The black dots (• • •), (••), (•) indicate a significance level of $p \leq 0.001$, $p \leq 0.01$, $p \leq 0.05$, respectively.

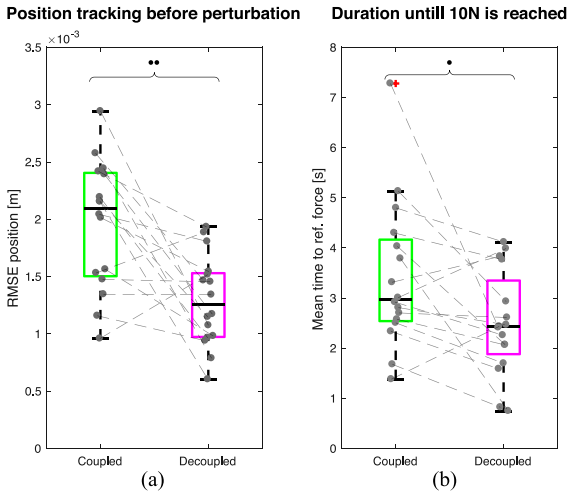

Fig. 9. (a) RMSE of the deviation from reference position before the force perturbation in the position tracking task is depicted on the most left. (b) Mean time to the reaching the reference force (i.e., from 0 N to 10 N) in the force tracking task is depicted on the right side. The coupled SCI is indicated by green color and the decoupled SCI by magenta color. Result of each individual participant is indicated by a grey dot. The within subject difference is represented by the grey dotted lines connecting the dots. The black dots (• • •), (••), (•) indicate a significance level of $p \leq 0.001$, $p \leq 0.01$, $p \leq 0.05$, respectively.

error in the force tracking task between the coupled SCI and decoupled SCI yielded a higher error when the coupled SCI was used. The difference was statistically significant $t(15) = 7.44$, $p \leq 0.001$. This is depicted in Fig. 8(b) and shown in Table III. The bottom-row graphs of Fig. 6 show time-series plots related to force tracking task for the coupled SCI and the decoupled SCI.

D. Double Task

Table IV shows the mean and SD for all dependent measures corresponding to the analysis of double task effect. In addition, the results of the paired-sample t-tests are reported. In the position tracking task, RMSE from the reference position was determined before the perturbation. Comparing RMSE position in the position tracking task between the coupled SCI and decoupled SCI yielded a higher error when the coupled SCI was used. The difference was statistically significant $t(15) = 3.68$, $p = 0.0022$. This is depicted in Fig. 9(a). In the force tracking task, the mean time to reference force (MTTRF) was determined. Comparing MTTRF in the force tracking task between the coupled SCI and decoupled SCI yielded a higher (worse) value

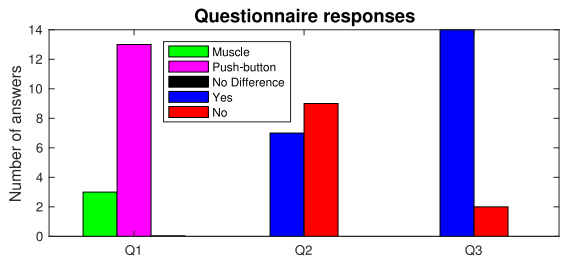

Fig. 10. Subjective measure results from the questionnaire.

when the coupled SCI was used. The difference was statistically significant $t(15) = 2.45$, $p = 0.0268$. This is depicted in Fig. 9(b). This difference in MTTRF of the force tracking task between the coupled SCI (green) and decoupled SCI (magenta) is also noticeable in the bottom-right graph of Fig. 6.

E. Subjective Analysis

The results from the postexperiment questionnaire show (see Fig. 10) that push-button was classified as more comfortable

to command stiffness. Furthermore, most participants did not perceive aid from the coupled SCI in keeping the reference position in the position tracking task. Almost all participants perceived aid from the decoupled SCI in keeping the reference force in the force tracking task.

V. Discussion

A. Main Results

This study introduced a concept called *coupling effect* and examined its influence on methods for slave robot stiffness commanding in a bilateral tele-impedance setup on a fundamental level. The results of the study highlighted different benefits and drawbacks of two common types of SCIs used in bilateral tele-impedance. These tradeoffs should be taken into consideration when applying different types of SCIs to different applications.

The coupled SCI allowed for statistically significantly better position tracking compared to using the decoupled SCI, when a perturbation disturbs the remote robot (and consequently the operator) unexpectedly. Mean absolute position error in the coupled and decoupled SCI condition during the perturbation in the position tracking task were 0.0242 and 0.0295 m, respectively. This can be attributed to the coupling effect, where human reflexes were exploited to help counteract the perturbation, since the operator's arm naturally stiffened up. Involuntary stiffening of the arm is a result of a rapid increase in muscle activity levels, which also yields a higher commanded stiffness to the remote robot. The increased stiffness of the remote robot makes the position tracking stricter according to the impedance control law and improves the task performance. Increasing the commanded stiffness with this speed cannot be achieved with the decoupled SCI because voluntary actions are much slower compared to reflexes [15]. This result confirms our hypothesis *H2*.

Mean absolute commanded stiffness error in the coupled and decoupled SCI condition during the perturbation in the position tracking task were 0.1194[-] and 0.0061[-], respectively. This difference was statistically significant. The larger error in the coupled SCI was a result of the coupling effect, where human reflexes stiffened operator's muscles in presence of perturbation. While this effect had a positive influence on position tracking, it negatively affected the commanded stiffness tracking. This result confirms our hypothesis *H1* with respect to the position tracking tasks.

The decoupled SCI allowed for statistically significantly better force tracking compared to using the coupled SCI, when remote robot is producing a reference force on an external object. Mean absolute force error (maintaining 10 N force for 4 s) in the coupled and decoupled SCI for the force tracking task were 1.1218 and 0.4303 N, respectively. The coupling effect adversely influenced the operator's ability to maintain a stable contact at the remote robot side. The contact produced fluctuations in force feedback, which operator perceived as small force perturbations, which in turn triggered reflexes that induced involuntary changes to commanded stiffness due to the coupling effect. This result confirms our hypothesis *H3*.

Mean absolute stiffness error in the coupled and decoupled SCI for the force tracking task were 0.0277[-] and 0.0067[-], for which the difference was statistically significant. As mentioned previously, the fluctuation in force feedback during the contact negatively affected the commanded stiffness tracking for the coupled SCI. This result confirms our hypothesis *H1* with respect to force tracking tasks.

Within the force tracking task, it was hypothesized that the coupling effect would be stronger when maintaining a constant force of 10 N compared to increasing (establishing) force from 0 to 10 N when using the coupled SCI. The small force perturbations of consistent magnitude, due to the nature of the stiffness signal, did not yield a statistically significant difference in absolute mean commanded stiffness error. This indicates that whenever the force does not change abruptly, the human operator was able to adapt to keep reference stiffness in the coupled SCI for both aspects of the force tracking task. Therefore, our hypothesis *H4* was not confirmed.

The original reasoning for *H4* was that maintaining a constant force (e.g, 10 N) is a much harder task than just pressing from zero to a certain force (e.g., from 0 to 10 N), therefore, the coupling effect may affect the reference stiffness commanding more for the force maintaining task. We had two underlying reasons for this. First, the higher force means larger force feedback perturbations at the master device that amplifies the coupling effect. Second, the force maintaining task may require more attention than just pressing from 0 to 10 N. Nevertheless, *H4* was rejected by the experiment results as there was no significant difference in the error of stiffness reference regulation between the maintaining stage and the pressing stage. However, some aspects of the reasoning behind *H4* might explain the higher SD of stiffness error during the maintaining stage compared to the pressing stage.

B. Subjective Analysis

Participants expressed that they were more comfortable in commanding stiffness with the decoupled SCI as it was easier to track reference stiffness with and took less effort. This can be attributed to muscle activity fluctuating with force feedback and reflexes. While the measurements showed that the coupling effect improved the position tracking task performance during perturbation, on average the participants did not subjectively perceive aid from the coupling effect in countering the position perturbation at the remote robot. However, on average the participants subjectively perceived aid in using the decoupled SCI to track the reference force, which is in line with the measurements.

C. Effect of Double Task

We also observed the effect of double task performance in the period prior to perturbation in the position tracking task, when the participants could focus entirely on controlling position and commanded stiffness of the remote robot. RMSE of the position in the coupled SCI condition was statistically significantly higher than in the decoupled SCI condition. The difference (0.0020 and 0.0013 m, respectively) can be attributed to the

notion that maintaining arm muscle activity is more difficult than maintaining a finger position on a push-button device.

In the force tracking task, MTTRF of the force signal in the coupled SCI condition was statistically significantly higher than in the decoupled SCI condition. This means that the participants could reach the reference force faster when using the decoupled SCI. The difference (3.4105 and 2.4886 s, respectively) can be attributed to more focus being required to keep the reference commanded stiffness in the coupled SCI condition, which tends the participant to approach the reference force more slowly.

We should note that maintaining reference commanded stiffness might not always be important in real-world scenarios, as long as the primary tasks (position/force tracking) are performed sufficiently on the remote robot side. For example, by using the coupled SCI, the operator can naturally perform the task based on the environmental interaction, while the stiffness automatically changes according to the coupling effect (as shown in the position tasking task with perturbation). If the dynamics of the human arm and the robot arm performing the task are comparable, using the coupled SCI can be intuitive and the coupling effect can be used as a natural aid. This can especially be beneficial when operator has to perform task with the remote robot under random impacts [2] or when visual feedback is limited or unavailable [18]. However, if the dynamics of slave and master are drastically different (e.g., operating a heavy-load robot or operating a microscopic surgical robot), the coupling effect may produce unnatural reactions.

Although commanding stiffness according to some reference is not something a typical interaction task requires, a practical example that does is found in tasks where a robotic arm has to interact with a very delicate object; such as glass in industrial tasks or human tissue/organ in surgical tasks. In such cases, it is important to command a prescribed safe low stiffness in order not to break or damage the delicate object. If the stiffness suddenly increases above the safe reference, as a result of the coupling effect, then the task cannot be performed in a safe manner.

D. Additional Aspects

We should note that the coupling effect only occurs when force feedback is present. That is, when a haptic interface is used to form a physical coupling with the human operator's arm [2], [8], [16], [18], [19]. The coupling effect is not present when there is no force feedback, since there is no physical coupling with the human arm. Such example are unilateral tele-impedance setups where the human arm is freely moving in the air and the commanded position is measured by optical sensors [5], [10], [21].

Another kind of interface used as stiffness command interface in bilateral tele-impedance setups is based on grip force [16], [17]. Various studies showed that grip force is highly correlated with the neuromuscular impedance [46], [47], therefore, with respect to the terminology of this study, commanding stiffness by grip force could be classified as coupled.

In the force tracking experiment, the wall appeared predictably and the subject had to approach it to establish the contact. If the wall appeared unexpectedly, the reflex effect would become more prominent. In this case, the condition would be similar to the condition of an object unexpectedly hitting the slave robot, as examined in the position tracking task.

We should stress that the main study was performed in absence of common real-world bilateral teleoperation issues (i.e., transparency, stability, etc.) in order to obtain uncorrupted results and to specifically examine the coupling effect on a fundamental level. This kind of a clean study can serve as a baseline for future studies regarding influences of specific bilateral teleoperation issues on the coupling effect. However, we performed analysis of transparency and stability mathematically in appendix (see Appendix), which indicate that the increased commanded stiffness of the slave robot due to the coupling effect can potentially destabilize the closed-loop stability, but on the other hand can temporarily improve the transparency of the system.

Other factors such as impedance estimation quality and expertise level of the operator could also influence the study. Since we were focused on the coupling effect itself, we strived to standardize the impedance estimation quality, expertise level of operators and other conditions as much as possible. In future, we will consider examining the effects of these two conditions.

The movements in the experiments were performed along the x-axis and were relatively small, therefore, an effect of arm configuration properties, such as manipulability, was not prominent. In future research, we will also consider examining the effect of (velocity and force) manipulability ellipsoids on the coupling effect.

In addition to proprioception and the sense of touch that are related to force feedback, human can also use other senses to perceive the remote environment in teleoperation. While this study focused primarily on the coupling effect of force feedback, visual and audio feedback might evoke reflexes too. Therefore, even unilateral tele-impedance or decoupled SCIs might be affected to some degree by other types of feedback. Future research will focus on whether or not the definition of the coupling effect could be extended to visual or audio feedback.

Next to reflexive muscle activity evoked by the force feedback of the system, we assumed that other cues, which could cause reflexive behavior (visual and audio), have negligible influence on the commanded stiffness signal in decoupled SCIs. However, it should be noted that in real-world settings, unexpected force perturbations at the primary limb (or at some other point of body) might elicit some reflex repose on the secondary limb too. In addition, other nonphysical cues (e.g., unexpected audio or visual cues) can potentially startle the operator and elicit reflexes on the secondary limb.

In this study, we used dichotomous scale in the questionnaire, which might have disadvantages compared to continuous scales. A continuous scale, like Likert 1–5 scale, gives more range, which is especially useful for information that is not easily quantifiable [35], [48]. Since *Q2* and *Q3* are already quantifiable by the actual measurements and act as a supplement to the main measured results, we selected the dichotomous scale and went for the smallest range to minimize the ambiguity. As for *Q1*, we preferred a binary answer to maximize the neutrality of the question, since continuous scales (e.g., Likert scale) may present a question-induced bias over the method preference.

VI. Conclusion

These novel fundamental insights in the coupling effect in bilateral tele-impedance should be an important consideration for users and applications. As a general guideline, we recommend using the coupled SCI for position tracking tasks, since the coupling effect can help to naturally counteract unexpected perturbations from the environment. On the other hand, we recommend using the decoupled SCI for scenarios where a contact should be established or where a specific interaction force should maintained, since results showed a better task performance with decoupled SCI. When scaling of the dynamics between the master and the slave is not comparable, the decoupled SCI might be preferred over the coupled SCI.

Appendix

In this appendix, we provide a mathematical tool and analysis of force feedback tele-impedance that specifically focuses on the coupling effect. Section VII-A examines transparency and Section VII-B examines stability. These properties have been extensively studied in the literature and various methods and solutions already exist [7], [11], [18], [23]–[25]. The purpose of this analysis is to highlight the novel insights and aspects specific to the coupling effect in force feedback tele-impedance.

A. Transparency

Transparency is one of the main performance measures for force feedback teleoperation, which indicates how well the system can transmit the remote environment impedance to the human operator [7], [49]. High transparency means that the human operator perceives very similar impedance at the master device, i.e. as if he/she was directly interacting with the remote environment. Low transparency means that the interaction at the master device is poorly reproduced. Transparency depends on system parameters (i.e., hardware, controller) and various conditions and factors. One of the key factors that can degrade transparency are time delays in the communication loop [7], [49].

We describe force feedback tele-impedance with the *hybrid matrix configuration* model [23], [25], which we modify to account for the coupling effect between the human impedance and the impedance of the slave controller (see Fig. 11). The relationship between the human force F_h and motion $\dot{x}_h$, and the remote environment force F_e and motion $\dot{x}_e$, is given by H matrix as

$$\begin{bmatrix} F_h \\ -\dot{x}_e \end{bmatrix} = \begin{bmatrix} h_{11} & h_{12} \\ h_{21} & h_{22} \end{bmatrix} \begin{bmatrix} \dot{x}_h \\ F_e \end{bmatrix} \tag{18}$$

where h_{11} is the input impedance, h_{22} is the output admittance, h_{21} is the motion scale, and h_{12} is the force scale.

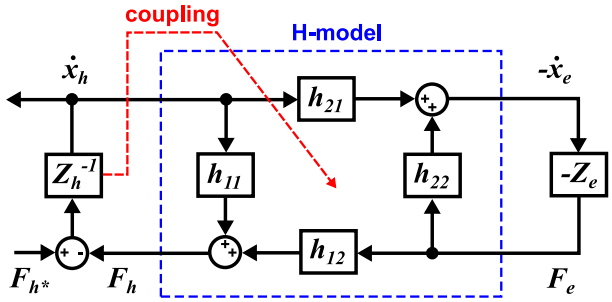

Fig. 11. H-model of a tele-impedance system. The specific modification from the standard model is signified by the red line, which indicates the coupling effect between the human impedance and the impedance of the slave controller. Z_h and Z_e are human and environment impedances, h_{11} and h_{22} are input impedance and output admittance, repetitively, and h_{21} and h_{12} are motion and force scales, respectively.

We use *multiple-input-multiple-output* formulation to describe the general control architecture as

$$\begin{bmatrix} F_{\text{mc}} \\ F_{\text{sc}} \end{bmatrix} = \begin{bmatrix} k_{11} & k_{12} & k_{13} & k_{14} \\ k_{21} & k_{22} & k_{23} & k_{24} \end{bmatrix} \begin{bmatrix} F_h & F_h \\ \dot{x}_h & \dot{x}_h \\ F_e & F_e \\ \dot{x}_e & \dot{x}_e \end{bmatrix} \tag{19}$$

where F_{mc} and F_{sc} are master and slave controller forces, repetitively, and $k_{i,j}(s)$ are controller transfer functions. Based on the elements $k_{i,j}$ of the controller matrix (19), the H matrix elements $h_{i,j}$ can be derived as [50]

$$h_{11} = \frac{(Z_m - k_{12})Z_s - k_{24}Z_m + k_{12}k_{24} - k_{14}k_{22}}{(k_{11}+1)Z_s + (-k_{11}-1)k_{24} + k_{14}k_{21}} \tag{20}$$

$$h_{12} = \frac{k_{13}Z_s - k_{13}k_{24} + k_{14}k_{23} - k_{14}}{(k_{11}+1)Z_s + (-k_{11}-1)k_{24} + k_{14}k_{21}} \tag{21}$$

$$h_{21} = \frac{k_{21}Z_m + (k_{11}+1)k_{22} - k_{12}k_{21}}{(k_{11}+1)Z_s + (-k_{11}-1)k_{24} + k_{14}k_{21}} \tag{22}$$

$$h_{22} = \frac{(k_{11}+1)k_{23} - k_{13}k_{21} - k_{11} - 1}{(k_{11}+1)Z_s + (-k_{11}-1)k_{24} + k_{14}k_{21}} \tag{23}$$

where Z_m and Z_s are the intrinsic impedances of master and slave devices, respectively.

The position-force control architecture, which was used in this study, is formulated as

$$\begin{bmatrix} F_{\text{mc}} \\ F_{\text{sc}} \end{bmatrix} = \begin{bmatrix} 0 & 0 & K_f e^{-sT_d} & 0 \\ 0 & \frac{K_s}{s}e^{-sT_d} & 0 & -\frac{K_s}{s} \end{bmatrix} \begin{bmatrix} F_h & F_h \\ \dot{x}_h & \dot{x}_h \\ F_e & F_e \\ \dot{x}_e & \dot{x}_e \end{bmatrix} \tag{24}$$

where K_s is the gain (stiffness) of the slave impedance controller [obtained from (9)] and K_f is the force feedback gain. T_d is a time delay in the communication loop, which is considered here for generality, even though the system in the main study had negligible delays. For formulations of other teleoperation architectures, refer to [11].

The modified H-model formulation that includes the coupling between the human impedance Z_h and the impedance of the slave controller K_s is, therefore, derived as

$$H(s) = \begin{bmatrix} Z_m & -K_f e^{-sT_d} \\ -\frac{K_s[Z_h]e^{-sT_d}}{sZ_s+K_s[Z_h]} & \frac{s}{sZ_s+K_s[Z_h]} \end{bmatrix} \tag{25}$$

where $K_s[Z_h]$ signifies the dependency that accounts for the specifics of the coupling effect during the reflex phase, when the human has no cognitive control over the arm impedance. This dependency has not been accounted for in analysis of standard force feedback teleoperation systems [7], [11], [23]–[25]. The formulation in (25) is specific to the system used in the study. Nevertheless, the formulation should be adapted if another teleoperation control architecture is employed (e.g., *position-position*, *position-force*, *4-channel*, etc. [7], [11], [23]–[25]), while accounting for the coupling effect similarly as in (25).

Deriving from H-model in (18) and assuming that there is no extra external force at the remote environment ($F_{e*} = 0$), the transmitted impedance from the environment to the human is defined as

$$Z_{th}(s) = \frac{F_h}{\dot{x}_h} = \frac{(h_{11}h_{22} - h_{12}h_{21})\, Z_e + h_{11}}{h_{22}Z_e + 1} \tag{26}$$

where Z_{th} is the impedance transmitted from the environment to the human via the master device. When there is no physical interaction with the remote environment (e.g., free air movement), the impedance of the environment is zero ($Z_e \to 0$) and the transmitted impedance at the master device becomes equal to that of the master device: $Z_{th,0} = h_{11} = Z_m$. Therefore, a master device with lighter hardware construction and better compensation of its dynamics, generally gives better transparency. The coupling effect has no influence on transparency in a free-air condition.

In the other extreme case, when the slave is interacting with a very stiff remote environment, like in the force tracking task on a wall in the experiments, we can examine the maximum possible impedance that can be transmitted by the system. This case is useful for the analysis since a very high impedance of remote environment is difficult to transmit and reproduce. Assuming the environment impedance goes to infinity ($Z_e \to \infty$) and deriving from (25), the transmitted impedance is approximately equal to

$$\begin{aligned} Z_{th,\infty}(s) &= \frac{h_{11}h_{22} - h_{12}h_{21}}{h_{22}} \\ &= \frac{sZ_m - K_f K_s[Z_h]e^{-s2T_d}}{s} \end{aligned} \tag{27}$$

where the transmitted stiffnesses in low and high frequency cases for a very stiff remote environment are

$$K_{th,\text{low}} = \lim_{s\to 0} sZ_{th,\infty}(s) = -K_f K_s[Z_h]e^{-s2T_d} \tag{28}$$

$$K_{th,\text{high}} = \lim_{s\to \infty} sZ_{th,\infty}(s) = sZ_m. \tag{29}$$

By examining (28), at low frequency one of the main transparency bottlenecks, which can degrade system performance, are time delays in the loop. At higher frequencies the time delay has an even larger negative effect on the transmitted impedance (i.e., the term $e^{-sT_d} = 1$ at $s = 0$ and exponentially decays as the frequency increases). Nevertheless, the coupling effect has no influence on time delays. Another potential limitation is the force feedback scaling factor K_f. Whenever it is set too low, the operator may not be able to sufficiently feel the interaction forces required to reproduce the desired impedance.

Nevertheless, the most interesting transparency limitation with respect to the paper's study is the slave controller impedance that is commanded by the human operator. In force feedback tele-impedance, the human operator feels the combined impedance of the environment and the slave robot, since the stiffness of the slave impedance controller scales the force feedback [2] [also seen in (28)]. In case of an interaction with a very stiff environment with low commanded stiffness of the slave impedance controller, the operator predominantly feels the compliance of the slave robot controller. This indicates that the commanded slave stiffness is also a limitation for transparency in tele-impedance [see $K_s[Z_h]$ in (28)]. Whenever an event induces a human operator's reflex, the stiffness value of K_s also increases through the coupling effect. This can temporarily improve transparency of the system in a low frequency case. On the other hand, by examining (29), the transmitted stiffness in a high frequency case is dominated by the master impedance. Therefore, the coupling effect does not have a significant influence on transparency.

B. Stability

Like any other force feedback teleoperation, force feedback tele-impedance is also prone to stability issues. Using the H-model from (18) in a closed-loop form and modified to include the coupling effect (see Fig. 11), we derive the closed-loop transfer function between human-induced external force F_{h*} and human arm (slave device) motion $\dot{x}_h$ as

$$\frac{\dot{x}_h}{F_{h*}} = \frac{h_{22}Z_e + 1}{(h_{22}Z_e + 1)\,(Z_h + h_{11}) - h_{12}h_{21}Z_e} \tag{30}$$

where H matrix elements, which include the gain (stiffness) of the slave impedance controller K_s, are dependent on Z_h. If the human impedance and the environment impedance are known, the derived closed-loop transfer function can be used to analyze the stability with the Root–Locus method [11], [24], [51] or the Nyquist method [7], [11], [51]. By varying the specific model parameters under set conditions, one can observe the stability margins of the corresponding tele-impedance system.

Previous studies on force feedback teleoperation have demonstrated that lower stiffness improves stability in teleoperation with a preset stiffness [11] and in tele-impedance with a human-commanded stiffness [2]. Within force feedback tele-impedance, increasing the commanded stiffness due to a human reflex as a result of the coupling effect can potentially destabilize the slave device; the poles of the closed-loop transfer function (30) might move into the right half-plane. Whether the stability limit is reached during the reflex depends on the parameters $h_{i,j}$ of any specific system (i.e., controller settings and human, hardware and environment dynamics) and various conditions and factors.

Another major stability factor are time delays in the teleoperation loop, where higher delays degrade the closed-loop

stability [7], [11], [52]. As seen from (24) and (25), delays in the communication loop effectively scale the parameters h_{12} and h_{21} and, therefore, influence the locations of closed-loop poles in (30). Nevertheless, the coupling effect has no influence on time delays.

REFERENCES

[1] H. Boessenkool, D. A. Abbink, C. J. Heemskerk, F. C. van derHelm, and J. G.Wildenbeest, "A task-specific analysis of the benefit of haptic shared control during telemanipulation," *IEEE Trans. Haptics*, vol. 6, no. 1, pp. 2–12, Jan.–Mar. 2012.

[2] L. Peternel, T. Petrič, and J. Babič, "Robotic assembly solution by human-in-the-loop teaching method based on real-time stiffness modulation," *Auton. Robots*, vol. 42, no. 1, pp. 1–17, 2018.

[3] T. B. Sheridan, "Human-robot interaction: Status and challenges," *Hum. Factors*, vol. 58, no. 4, pp. 525–532, 2016.

[4] B. S. Peters, P. R. Armijo, C. Krause, S. A. Choudhury, and D. Oleynikov, "Review of emerging surgical robotic technology," *Surg. Endoscopy*, vol. 32, no. 4, pp. 1636–1655, 2018.

[5] L. Peternel, T. Petrič, E. Oztop, and J. Babič, "Teaching robots to cooperate with humans in dynamic manipulation tasks based on multi-modal human-in-the-loop approach," *Auton. Robots*, vol. 36, no. 1/2, pp. 123–136, 2014.

[6] L. Peternel, E. Oztop, and J. Babič, "A shared control method for online human-in-the-loop robot learning based on locally weighted regression," in *Proc. IEEE/RSJ Int. Conf. Int. Robots Syst.*, 2016, pp. 3900–3906.

[7] D. A. Lawrence, "Stability and transparency in bilateral teleoperation," *IEEE Trans. Robot. Autom.*, vol. 9, no. 5, pp. 624–637, Oct. 1993.

[8] L. Peternel, T. Petrič, and J. Babič, "Human-in-the-loop approach for teaching robot assembly tasks using impedance control interface," in *Proc. IEEE Int. Conf. Robot. Autom.* , 2015, pp. 1497–1502.

[9] W. S. Kim, B. Hannaford, and A. Fejczy, "Force-reflection and shared compliant control in operating telemanipulators with time delay," *IEEE Trans. Robot. Autom.*, vol. 8, no. 2, pp. 176–185, Apr. 1992.

[10] A. Ajoudani, N. Tsagarakis, and A. Bicchi, "Tele-impedance: Teleoperation with impedance regulation using a body-machine interface," *Int. J. Robot. Res.*, vol. 31, no. 13, pp. 1642–1656, 2012.

[11] G. A. Christiansson and F. C. Van DerHelm, "The low-stiffness teleoperator slave-a trade-off between stability and performance," *Int. J. Robot. Res.*, vol. 26, no. 3, pp. 287–299, 2007.

[12] E. Burdet, R. Osu, D. W. Franklin, T. E. Milner, and M. Kawato, "The central nervous system stabilizes unstable dynamics by learning optimal impedance," *Nature*, vol. 414, no. 6862, pp. 446–449, 2001.

[13] C. Yang, G. Ganesh, S. Haddadin, S. Parusel, A. Albu-Schaeffer, and E. Burdet, "Human-like adaptation of force and impedance in stable and unstable interactions," *IEEE Trans. Robot.*, vol. 27, no. 5, pp. 918–930, Oct. 2011.

[14] N. Hogan, "Adaptive control of mechanical impedance by coactivation of antagonist muscles," *IEEE Trans. Autom. Control*, vol. 29, no. 8, pp. 681–690, Aug. 1984.

[15] D. A. Abbink, M. Mulder, F. C. Van der Helm, M. Mulder, and E. R. Boer, "Measuring neuromuscular control dynamics during car following with continuous haptic feedback," *IEEE Trans. Syst., Man, Cybern., B*, vol. 41, no. 5, pp. 1239–1249, Oct. 2011.

[16] D. S. Walker, R. P. Wilson, and G. Niemeyer, "User-controlled variable impedance teleoperation," in *Proc. IEEE Int. Conf. Robot. Autom*., 2010, pp. 5352–5357.

[17] D. S. Walker, "Design of versatile telerobotic systems using variable impedance actuation and control," Ph.D. dissertation, Dept. Mech. Eng., Stanford University, Stanford, CA, USA, 2013.

[18] M. Laghi, A. Ajoudani, M. G. Catalano, and A. Bicchi, "Unifying bilateral teleoperation and tele-impedance for enhanced user experience," *Int. J. Robot. Res.*, vol. 39, no. 4, pp. 514–539, 2020.

[19] C. Yang, C. Zeng, P. Liang, Z. Li, R. Li, and C. Su, "Interface design of a physical human-robot interaction system for human impedance adaptive skill transfer," *IEEE Trans. Autom. Sci. Eng.*, vol. 15, no. 1, pp. 329–340, Jan. 2018.

[20] E. Zheng, Y. Li, Q. Wang, and H. Qiao, "Toward a human-machine interface based on electrical impedance tomography for robotic manipulator control," in *Proc. IEEE/RSJ Int. Conf. Int. Robot. Syst.*, Nov. 2019, pp. 2768–2774.

[21] A. Ajoudani, C. Fang, N. Tsagarakis, and A. Bicchi, "Reduced-complexity representation of the human arm active endpoint stiffness for supervisory control of remote manipulation," *Int. J. Robot. Res.*, vol. 37, no. 1, pp. 155–167, 2018.

[22] L. M. Doornebosch, D. A. Abbink, and L. Peternel, "The force-feedback coupling effect in bilateral tele-impedance," in *Proc. 8th IEEE RAS/EMBS Int. Conf. Biomed. Robot. Biomechatronics,*2020, pp. 152–157.

[23] B. Hannaford, "A design framework for teleoperators with kinesthetic feedback," *IEEE Trans. Robot. Autom.*, vol. 5, no. 4, pp. 426–434, Aug. 1989.

[24] R. Daniel and P. R. McAree, "Fundamental limits of performance for force reflecting teleoperation," *Int. J. Robot. Res.*, vol. 17, no. 8, pp. 811–830, 1998.

[25] K. Hashtrudi-Zaad and S. E. Salcudean, "Analysis of control architectures for teleoperation systems with impedance/admittance master and slave manipulators," *Int. J. Robot. Res.*, vol. 20, no. 6, pp. 419–445, 2001.

[26] N. Hogan, "Impedance control: An approach to manipulation: Part ii-implementation," *J. Dyn. Syst., Measurement, Control*, vol. 107, no. 1, pp. 8–16, 1985.

[27] A. Albu-Schäffer, C. Ott, and G. Hirzinger, "A unified passivity-based control framework for position, torque and impedance control of flexible joint robots," *Int. J. Robot. Res.*, vol. 26, no. 1, pp. 23–39, 2007.

[28] T. Tsuji, P. G. Morasso, K. Goto, and K. Ito, "Human hand impedance characteristics during maintained posture," *Biol. Cybern.*, vol. 72, no. 6, pp. 475–485, 1995.

[29] H. Gomi and R. Osu, "Task-dependent viscoelasticity of human multijoint arm and its spatial characteristics for interaction with environments," *J. Neurosci.*, vol. 18, no. 21, pp. 8965–8978, 1998.

[30] H. Patel, G. ONeill, and P. Artemiadis, "On the effect of muscular cocontraction on the 3-d human arm impedance," *IEEE Trans. Biomed. Eng.*, vol. 61, no. 10, pp. 2602–2608, Oct. 2014.

[31] K. P. Tee, E. Burdet, C.-M. Chew, and T. E. Milner, "A model of force and impedance in human arm movements," *Biol. Cybern.*, vol. 90, no. 5, pp. 368–375, 2004.

[32] S. K. Charles and N. Hogan, "Dynamics of wrist rotations," *J. Biomech.*, vol. 44, no. 4, pp. 614–621, 2011.

[33] A. W. Peaden and S. K. Charles, "Dynamics of wrist and forearm rotations," *J. Biomech.*, vol. 47, no. 11, pp. 2779–2785, 2014.

[34] A. V. Hill, "The heat of shortening and the dynamic constants of muscle," *Proc. Roy. Soc. London. Ser. B-Biol. Sci.*, vol. 126, no. 843, pp. 136–195, 1938.

[35] L. Peternel, C. Fang, N. Tsagarakis, and A. Ajoudani, "A selective muscle fatigue management approach to ergonomic human-robot comanipulation," *Robot. Comput.-Integr. Manuf.*, vol. 58, pp. 69–79, 2019.

[36] N. Karavas, A. Ajoudani, N. Tsagarakis, J. Saglia, A. Bicchi, and D. Caldwell, "Tele-impedance based stiffness and motion augmentation for a knee exoskeleton device," in *Proc. IEEE Int. Conf. Robot. Autom.*, 2013, pp. 2194–2200.

[37] A. Ajoudani *et al.*, "Exploring teleimpedance and tactile feedback for intuitive control of the pisa/iit softhand," *IEEE Trans. Haptics*, vol. 7, no. 2, pp. 203–215, Apr.–Jun. 2014.

[38] A. Ajoudani, C. Fang, N. G. Tsagarakis, and A. Bicchi, "A reduced-complexity description of arm endpoint stiffness with applications to teleimpedance control," in *Proc. IEEE/RSJ Int. Conf. Intell. Robot. Syst.,* 2015, pp. 1017–1023.

[39] L. Peternel, N. Tsagarakis, and A. Ajoudani, "A human-robot comanipulation approach based on human sensorimotor information," *IEEE Trans. Neural Syst. Rehabil. Eng.*, vol. 25, no. 7, pp. 811–822, Jul. 2017.

[40] A. Ajoudani, N. G. Tsagarakis, and A. Bicchi, "Choosing poses for force and stiffness control," *IEEE Trans. Robot.*, vol. 33, no. 6, pp. 1483–1490, Dec. 2017.

[41] A. Albu-Schaffer, C. Ott, U. Frese, and G. Hirzinger, "Cartesian impedance control of redundant robots: Recent results with the dlr-light-weight-arms," in *Proc. IEEE Int. Conf. Robot. Autom.*, 2003, vol. 3, pp. 3704–3709.

[42] M. Ferre, R. Aracil, C. Balaguer, M. Buss, and C. Melchiorri, Advances in Telerobotics. Berlin, Germany: Springer, 2007, vol. 31.

[43] H. J. Hermens *et al.*, "European recommendations for surface electromyography," *Roessingh Res. Develop.*, vol. 8, no. 2, pp. 13–54, 1999.

[44] W. J. Conover and R. L. Iman, "Rank transformations as a bridge between parametric and nonparametric statistics," *Amer. Statistician*, vol. 35, no. 3, pp. 124–129, 1981.

[45] R. A. Armstrong, "When to use the b onferroni correction," *Ophthalmic Physiol. Opt.*, vol. 34, no. 5, pp. 502–508, 2014.

[46] H. Nakamura, D. Abbink, and M. Mulder, "Is grip strength related to neuromuscular admittance during steering wheel control?" in *Proc. IEEE Int. Conf. Syst., Man, Cybern*., 2011, pp. 1658–1663.

[47] A. Pronker, D. Abbink, M. Van Paassen, and M. Mulder, "Estimating driver time-varying neuromuscular admittance through lpv model and grip force," IFAC-PapersOnLine, vol. 50, no. 1, pp. 14 916–14921, 2017.
[48] S. Fani *et al.*, "Simplifying telerobotics: Wearability and teleimpedance improves human-robot interactions in teleoperation," *IEEE Robot. Autom. Mag.*, vol. 25, no. 1, pp. 77–88, Mar. 2018.
[49] J. E. Colgate and J. M. Brown, "Factors affecting the z-width of a haptic display," in *Proc. IEEE Int. Conf. Robot. Autom.*, 1994, pp. 3205–3210.
[50] G. A. V. Christiansson, "Hard master, soft slave haptic teleoperation," Ph.D. dissertation, Dept. Biomech. Eng., TU Delft, Delft, The Netherlands, 2007.
[51] K. Ogata, Modern Control Engineering, *5th ed.*, Englewood Cliffs, NJ, USA: Prentice-Hall, 2009.
[52] G. Niemeyer and J.-J. E. Slotine, "Telemanipulation with time delays," *Int. J. Robot. Res.*, vol. 23, no. 9, pp. 873–890, 2004.

Luuk Maria Doornebosch received the bachelor's degree from Delft University of Technology, Delft, The Netherlands, in 2017, and the master's degree from the Department of Cognitive Robotics, Delft University of Technology, in 2019, both in mechanical engineering.

David A. Abbink (Senior Member, IEEE) received the M.Sc. and Ph.D. degrees in mechanical engineering from the Delft University of Technology, Delft, The Netherlands, in 2002 and 2006, respectively.

He is currently a Full Professor in Delft, where he leads the Human-Robot Interaction group of the Cognitive Robotics Department. His research interests include human motor control, bilateral telemanipulation, haptic assistance and shared control.

Dr. Abbink was the recipient of two prestigious personal grants - VENI (2010) and VIDI (2015) - on haptic shared control for telerobotics and vehicle control. He is a Co-Founder of the IEEE SMC Technical Committee on Shared Control.

Luka Peternel (Member, IEEE) received the Ph.D. degree in robotics from the University of Ljubljana, Ljubljana, Slovenia, in 2015.

He conducted Ph.D. studies with the Department for Automation, Biocybernetics and Robotics, Jožef Stefan Institute in Ljubljana, Ljubljana, from 2011 to 2015, and with the Department of Brain-Robot Interface, ATR Computational Neuroscience Laboratories in Kyoto, Japan, in 2013 and 2014, respectively. He was with the Human-Robot Interfaces and Physical Interaction Lab of Italian Institute of Technology in Genoa, Italy from 2015 to 2018. From 2019, he is with the Department of Cognitive Robotics, Delft University of Technology in the Netherlands. His research interests include physical human-robot interaction, teleoperation and human motor control.